PULSED LASER DEPOSITION OF (Ba,Sr)TiO$_3$ FERROELECTRIC THIN FILMS

J.S. HORWITZ, W. CHANG, A.C. CARTER, J.M. POND, S.W. KIRCHOEFER, D.B. CHRISEY, R.M. STROUD, J. LEVY[a] AND C. HUBERT[a]
Naval Research Laboratory, Washington D.C., 20375-5345
[a]Department of Physics and Astronomy, University of Pittsburgh

ABSTRACT

Single phase, (100) oriented $Ba_{0.5}Sr_{0.5}TiO_3$ (BST) thin films have been deposited onto (100) $LaAlO_3$, $SrTiO_3$, and MgO substrates using pulsed laser deposition (PLD). Interdigitated capacitors patterned on top of the ferroelectric film have been used to measure the dielectric constant and dissipation factor of these films as a function of DC bias and temperature at 1 MHz and as a function of DC bias and frequency (1 to 20 GHz) at room temperature. At room temperature, the capacitance can be reduced by as much as a factor of 4 using an electric field of ≤ 80 kV/cm. The dielectric properties (% tuning and dielectric loss) of the ferroelectric film is sensitive to both the deposition and post processing conditions. Optical imaging of the ferroelectric films using confocal scanning optical microscopy (CSOM) shows reproducible polarization fluctuations over sub-micrometer length scales. Dielectric loss in the ferroelectric film is reduced through a combination of post deposition processing and donor/acceptor doping of the films. A zero field $\tan\delta = 0.01 - 0.005$ has been measured for BST films which show significant tuning at microwave frequencies.

INTRODUCTION

Ferroelectric materials offer unique opportunities for the development of tunable microwave signal processing devices[1]. In a ferroelectric, the dielectric constant can be reduced by the application of a DC electric field. This phenomena has been referred to as the dielectric non-linearity. The field dependent change in the dielectric constant can be used to modify the transport of electromagnetic energy. For a resonant structure, this causes a shift in the resonant frequency and for a transmission line, this causes a variable delay. There is substantial work currently being done on the development of tunable microwave devices based on ferroelectric materials. This work is being done primarily on $SrTiO_3$ and $Ba_xSr_{1-x}TiO_3$ because both materials have high dielectric constants and large electric field responses. The required electric fields (≤ 200 kV/cm) serve as a strong motivation to implement tunable microwave device structures in thin films where the bias voltages can be ≤ 10 V.

Examples of microwave devices that could be fabricated from ferroelectric thin films include tunable bandpass and band-reject filters, tunable oscillators delay lines and phase shifters. The ferroelectric film can be used in either a coplanar or microstrip geometry. These devices are used in a broad spectrum of microwave communication and radar systems. Ferroelectric thin film based devices offer the potential for light weight, low power replacement parts for semiconducting based devices with significantly improved device figures of merit in addition to the development of new device concepts. There are two fundamental parameters that characterize the performance of a ferroelectric material for a tunable

Mat. Res. Soc. Symp. Proc. Vol. 526 © 1998 Materials Research Society

microwave device. These are the relative change in the dielectric constant for a given applied electric field (E) (% tuning = $\varepsilon(E)/\varepsilon(0)$) and the loss tangent ($\tan\delta$) at zero field. For microwave applications, a large change in the dielectric constant ($\geq$ 50%) and low dielectric loss ($\tan\delta \leq 10^{-3}$) are required.

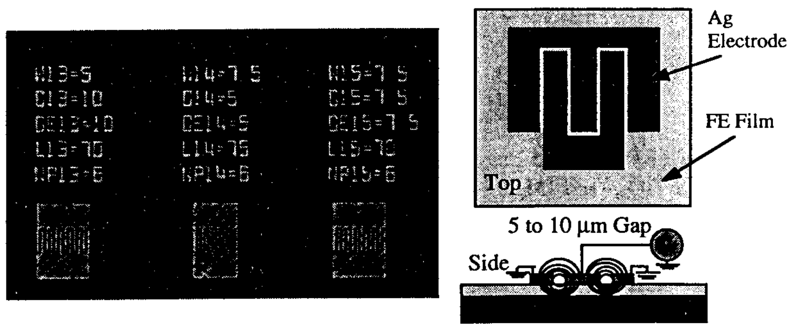

Figure 1 - Interdigitated capacitor used to measure dielectric properties of ferroelectric thin films.

EXPERIMENTAL

High quality BST thin films were deposited using pulsed laser deposition (PLD)[2,3]. The output of a short pulse excimer laser (248 nm, 30 ns FWHM) is focused on the target to an energy density of 1 - 2 J/cm^2. The BST targets were made from $BaTiO_3$ and $SrTiO_3$. The powders were mixed in a mechanical shaker for 30 minutes and pressed into the form of a pellet that is one inch in diameter under 2000 pounds for 15 minutes. The pressed pellets were then dried and calcined in Pt foil at 800° C for 4 hours, crushed, repressed and sintered in Pt foil at 1350° C for 6 hours. Chemical analysis of the films was performed by inductively coupled plasma spectroscopy (ICP) and electron-beam microprobe analysis to determine the elemental ratios of Ba, Sr, and Ti.

For annealing temperatures below 1050 °C, BST films were post-deposition annealed in flowing O_2. Films annealed above 1050° C were done in a BST vessel that was wrapped in platinum foil and placed in an alumna tube. The tube was capped at both ends, flushed with O_2 before annealing and maintained at a slight positive pressure of O_2 during the annealing process.

All films were characterized by x-ray diffraction (XRD) and representative films were coated with 500 Å of Au/Pt for scanning electron microscopy (SEM). Interdigitated capacitors, shown in Figure 1, were deposited on top of the FE films through a PMMA lift off mask by e-beam evaporation of 1-2 μm thick Ag and a protective thin layer of Au. Interdigitated capacitors had finger lengths of 10 to 100 μm with gaps that ranged from 5 to 15 μm. One to twenty GHz microwave measurements were made on an HP 8510 network analyzer between 1 and 20 GHz at room temperature. Temperature dependent measurements were performed at 1 MHz using a HP 4285A Precision LCR Meter.

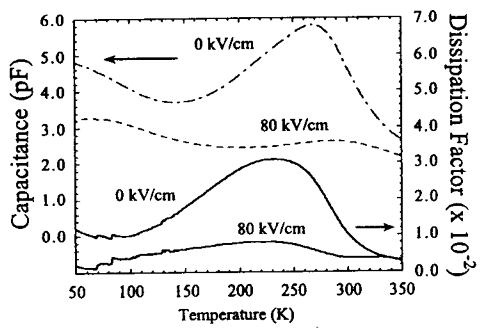

Figure 2 - Temperature dependence of capacitance and dissipation factor for a $Ba_{0.5}Sr_{0.5}TiO_3$ thin film capacitor measured at 1 MHz.

DIELECTRIC CHARACTERIZATION

The temperature dependence of the capacitance and dissipation factor measured at 1 MHz for an interdigitated ferroelectric capacitor is shown in Figure 2. The peak in the capacitance curve corresponds to the phase transition between the paraelectric and ferroelectric phases (T_c). The dielectric loss exhibits a temperature dependence reaching a maximum at a temperature slightly lower than T_c. When a DC field is placed across the capacitor, the dielectric constant is reduced. In general, the dielectric properties of the films are different from the corresponding bulk material. The temperature dependence of the dielectric constant and dissipation factor for the film are much broader than the bulk (by about a factor of 6)[4] and the dielectric constant is lower by about a factor of 5 [5].

K-Factor

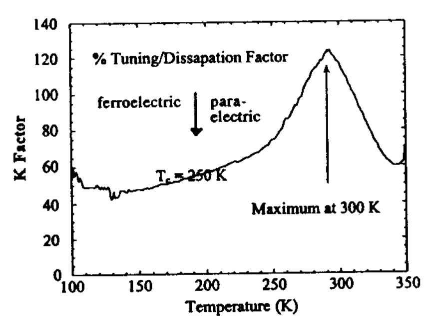

Figure 3 - Calculated K-factor for 80 kV/cm for $Ba_{0.5}Sr_{0.5}TiO_3$ thin film capacitor as a function of temperature measured at 1 MHz.

A single figure of merit is often used to measure the quality of the thin film material for microwave tunable applications. A K-factor is defined as the ratio of the % change in the capacitance for a given applied field divided by the dielectric loss. It is shown in Figure 3 for a BST (x=0.5) thin film ferroelectric interdigitated capacitor. Large K-factors correspond to a large tuning range and/or low dielectric loss. The K factor for this BST film is at a maximum just above the Curie temperature (T_c). The T_c for BST (x=0.5) is ~ 250 K. It is therefore necessary to remain just to the paraelectric side of T_c to have a low loss oscillator with a large dynamic range. To achieve intrinsic dielectric loss in BST materials will require materials with a low defect density. Typically, the lowest defect density is observed in single crystals. Only $BaTiO_3$ and $SrTiO_3$ are readily available as single crystals.

The dielectric properties for BST ferroelectric thin films have been measured at room temperature between 1 - 20 GHz. As-deposited films exhibit a large electric field dependence. Capacitance changes as large as 4:1 for fields ≤ 80 kV/cm (Figure 4). As-deposited films have relatively high dielectric loss. At zero bias, dielectric Q's (~1/tanδ) of 5 - 20 are typical. The Q is strongly dependent on the electric field which increased (meaning a decrease in tanδ) as the electric field increased. There are several sources existing of dielectric loss in the ferroelectric films including stoichiometric deficiencies which create vacancies (cation and anion), film strain (due to the lattice mismatch between the film and the substrate), and the presence of small grains (resulting a large grain boundary/grain ratio). To reduce the dielectric loss, as-deposited films were post-annealed in flowing oxygen. The post-deposition anneal was designed to remove film strain by filling oxygen vacancies and increase the overall grain size of the dielectric film.

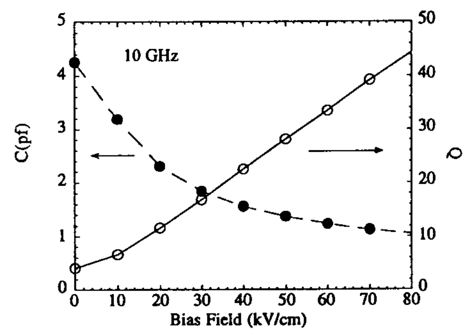

Figure 4 - Electric field dependence of FE capacitor measured at 298 K at 10 GHz.

POST DEPOSITION PROCESSING OF FE FILMS

Oxygen (anion) vacancies are present in films deposited in a relatively low partial pressure of oxygen (~300 mTorr). To remove oxygen vacancies, PLD thin films have been post-annealed in flowing oxygen at temperatures from 900 °C to 1350 °C. After annealing the as-deposited films, significant changes were observed in the structure and dielectric properties. X-ray diffraction of the post-annealed films indicates a decrease in the lattice parameter (presumably due to filling of oxygen vacancies) and a decrease in non-uniform strain[6]. The influence of the post-deposition anneal can be seen clearly in several aspects of the capacitance and dissipation factor as a function of temperature. In the capacitance data, we see the temperature dependence of the dielectric constant, approaching more bulk-like behavior. Second, we see a shift in the Curie temperature of the film. The T_c is increased by about 25 K. In general, annealing of the BST films produces films with more bulk like behavior.

As-deposited BST films are smooth and have a grain size of ~250 Å as observed by scanning electron microscopy (SEM). After annealing at 900° C for 8 hours, the films were smoother but the surface topology still suggested grain boundaries underneath. Annealing at temperatures above 1000° C in flowing O_2 resulted in surface coarsening such that the films could no longer be patterned for devices. The films became cloudy to the eye and showed what appeared to be erosion at the grain boundaries, revealing a 20 fold increase in grain size from the as deposited films (Figure 5a).

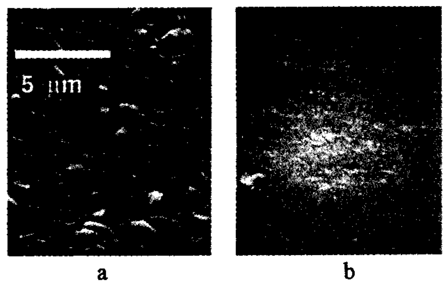

Figure 5 - SEM photomicrograph of oxygen annealed (a) and bomb annealed (b) BST thin film .

Using a ceramic "bomb" (Figure 6). to increase the partial pressure of the volatile elements in the vapor surrounding the film completely stopped the grooving around the grains and allowed annealing[7] temperatures of 1250° C while the films maintained a smooth surface that revealed no grain boundaries (The bomb is the bulk ceramic target material which surrounds the film during the high temperature, post-deposition anneal).

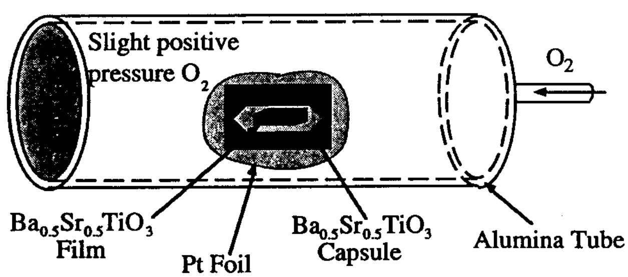

Figure 6 "Bomb" annealing of ferroelectric thin films.

CSOM

PLD thin films of BST have been examined using confocal scanning optical microscopy (CSOM)[8]. The high sensitivity ($\Delta n/n \sim 10^{-7}$) and high spatial resolution of this technique (<0.5 μm) could help to identify factors contributing to dielectric loss. In CSOM, electric field-induced reflectivity changes in the thin film arise from the linear electro-optic effect, whose coefficient is proportional to the spontaneous ferroelectric polarization P_s. The reflected light intensity r is modulated at the frequency of the driving field, and detected with a lock-in amplifier.

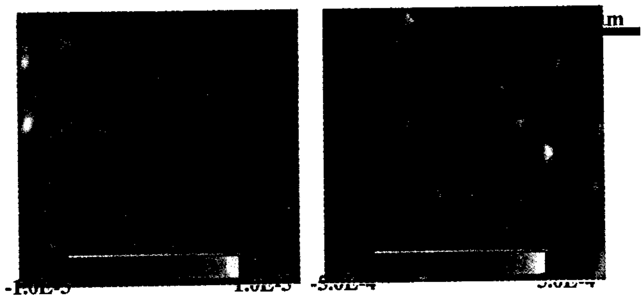

a b

Figure 7 CSOM images of $Ba_{0.5}Sr_{0.5}TiO_3$ films grown on (a) MgO and (b) $SrTiO_3$, taken at zero bias. Image area is $(7\mu m)^2$ for each sample.

The ferroelectric polarization image is obtained by raster-scanning the sample at a fixed dc electric field. In this way, it is possible to track the re-orientation of ferroelectric domains as a function of the applied field. In the second mode, the dc electric field from the interdigitated capacitor is slowly swept while acquiring data at a fixed point on the sample. These traces yield information about the local hysteretic behavior of the sample. Fig. 7a shows a CSOM image of a $Ba_{0.5}Sr_{0.5}TiO_3$ film at zero bias grown on an MgO substrate. Fig. 7b shows a CSOM image of a $Ba_{0.5}Sr_{0.5}TiO_3$ film grown on $SrTiO_3$. Both images show reproducible polarization fluctuations over sub-micrometer length scales, but the film grown on $SrTiO_3$ exhibits a much larger signal (x50). The application of a dc bias reveals further differences between the two samples. CSOM images of the same $Ba_{0.5}Sr_{0.5}TiO_3$ sample as in Fig. 6b, in which E_{dc} is varied from -30 kV/cm to +30 kV/cm and back show a large number of micron-sized domains that flip their orientation. The coercive field is comparable to what is observed in bulk $BaTiO_3$ (~1-2 kV/cm). Surprisingly, a number of regions re-orient *opposite* to the applied field. In these samples, one can observe many localized regions of hysteresis. These regions are interspersed with areas which are not hysteretic.

DOPING AND STRAIN

Table 1 Composition of BSTFilms

	. Ba (atomic ratio)	Sr (atomic ratio)	Ti (atomic ratio)
Theoretical Bulk	0.500	0.500	1.000
Electron-beam Microprobe Flourescence	0.478 ±0.020	0.467 ±0.020	1.000 (normalized)
ICP	0.478 ±0.020	0.456 ±0.020	1.000 (normalized)

Improvements in the dielectric properties (i.e., increase in tuning and dielectric Q) of the annealed BST films have been found through the use of two types of dopants, compensation and donor acceptor dopants[9]. Non-stoichiometry is a known defect and affects various properties in ferroelectric materials[10,11]. The most common defect structure in $Ba_xSr_{1-x}TiO_3$ and $SrTiO_3$ are the doubly ionized oxygen vacancies, caused by loss of oxygen, cation off-stoichiometry (missing Ba or Sr) or impurities, which create free carriers in order to maintain charge neutrality[10,12-16]. The soft mode frequency in $SrTiO_3$ increases when the oxygen vacancy concentration increases[17]. The hardening of the soft-mode phonon will influence the ferroelectric tunability and loss. Annealing of oxygen deficient film at high temperatures in flowing oxygen results in an increase in the oxygen content and a reduction in the dielectric loss[6].

Chemical analysis of the PLD BST films (Table 1) shows they exhibit measurable cation vacancies which are as much as ~6% deficient in Ba and Sr. Increasing the amount of available Ba and Sr was achieved by compensating the targets with excess metal oxides. Initial measurements in which the target was compensated with an additional 2 % Ba and Sr did not show a significant increase of Ba and Sr content of the deposited films, but it did result in ~60% improvement in dielectric loss compared to uncompensated films.

It is possible that the stoichiometry of the film may have a fixed deficiency in Ba and Sr due to surface effects at grain boundaries. As-deposited films show columnar structure. Each grain is a column approximately 125 Å in radius. Each unit cell is approximately 4 Å in size. Assuming that the BST grain is coated with a material that is deficient in Ba and Sr. If all the missing Ba and Sr material were at the grain boundary then the boundary layer would consist of pure TiO_2. Assuming a single unit cell layer of TiO_2, that gives the grain an inner core of 121 Å and an outer surface layer of 4 Å. The outer layer represents 7 % of the total volume. This could account entirely for the Ba and Sr deficiency observed in the as-deposited films. To achieve stoichiometric films will require techniques that can alter the grain size of the as deposited film. To increase the grain size will require greater surface mobility of the arriving vapor atoms at the substrate surface which can be achieved both by raising the substrate deposition temperature and/or reducing the oxygen deposition temperature.

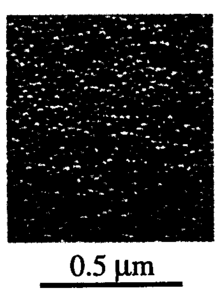

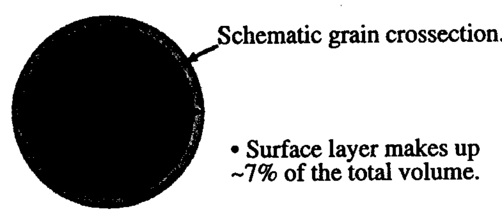

Figure 8 SEM photomicrograph of BST thin film showing columnar microstructure.

One of the most important factors inherently associated with hetero-epitaxial thin films is strain. Due to the lattice mismatch between the film and the substrate and the different thermal expansion coefficients, thin films are subject to various degrees of strain[18].

The cubic lattice parameters for MgO, $SrTiO_3$ and $LaAlO_3$ are 4.213, 3.905, 3.787 Å, respectively. This yields a lattice mismatch for $Ba_{0.5}Sr_{0.5}TiO_3$ of ~1% for films deposited onto $SrTiO_3$ to about 7% for films deposited onto MgO. The large lattice mismatch, even for BST on $SrTiO_3$, can create significant strain at the film substrate interface leading to the production of structural defects. In terms of strain effects on microwave tunability, experiments showed that the tunability decreases when an increasing hydrostatic pressures is applied to an $SrTiO_3$ single crystal[19]. In $Ba_xSr_{1-x}TiO_3$ thin films, the microwave loss tangent increases with increasing strain[20] and is associated with films substrate lattice mismatch. Strain can also result in the formation of a ferroelectric phase transition in non-ferroelectric materials. Localized strain can result in localized region of ferroelectric behavior (higher loss) in an otherwise paraelectric (low loss) film. Shown in Figure 9 is a high resolution, cross section transmission electron micrograph of a BST film grown by PLD on an MgO substrate. The TEM micrograph shows a region at the interface that exhibits significant disorder. However, above the interface, the film is highly ordered. Above the disordered interface, there appears to be some variation in the orientation of the film of the film with respect to the substrate. This could be an indication of the texturing normally observed in these film (x-ray ω scan widths are typically 0.1 - 0.5° FWHM) or the presence of grains with orientations other than the [100] normal to the substrate surface. The disorder region pay provide a mechanism for strain relief between the film and the non-lattice matched substrate.

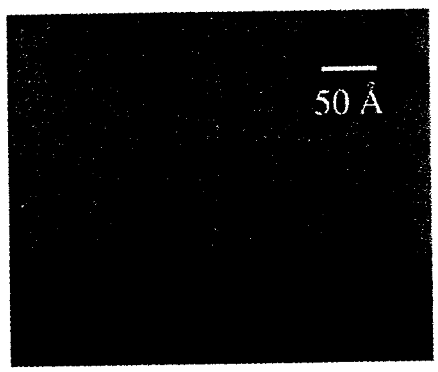

Figure 9 High resolution cross section TEM of BST thin film deposited onto MgO

Conductivity loss due to the presence of free carriers can be high in reduced or impurity doped ferroelectric materials[21,22]. Small amounts of impurities[10] can generate oxygen vacancies. Free carrier absorption could contribute substantially to microwave losses[22]. It is possible that doping with foreign ions can compensate for the presence of free carriers[14]. Doping $Ba_xSr_{1-x}TiO_3$ with a small amount (≤ 1 mole %) of acceptor dopant has been demonstrated to lower its loss tangent from 0.01 to 0.003[23]. Mn and Fe have been shown to significantly reduce the dielectric loss in bulk BST[24]. Mn acts as an acceptor impurity at the grain boundary[25]. Mn^{+3} ions can also substitute for Ti^{+4} ion and behave as electron acceptors. The Mn prevents reduction of Ti^{+4} to Ti^{+3} by neutralizing oxygen vacancies caused by low oxygen pressures. The microwave loss caused by free carrier absorption is proportional to the conductivity and inversely proportional to the frequency. Shown in Figures 10 are the dielectric measurements for a Mn-doped (1-2 atomic percent) $Ba_{0.5}Sr_{0.5}TiO_3$ film which has been bomb annealed. A 30% change in the capacitance is observed for an applied field of 67 kV/cm (40V bias over a 6 μm gap). Dielectric Qs are ~100 over the entire frequency range. In addition, the dielectric loss is relatively insensitive to the applied electric field.

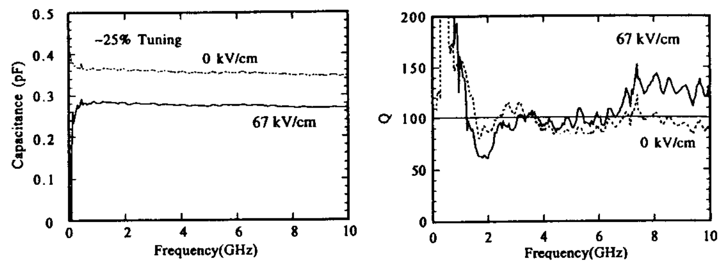

Figure 10 - Capacitance and dielectric Q for SBT film measured from 1 - 10 GHz at room temperature.

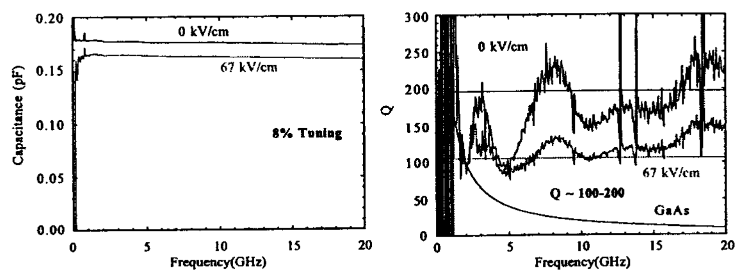

Figure 11 - Capacitance and dielectric Q for SBT film measured from 1 - 10 GHz at room temperature.

The dielectric properties of another BST capacitor is shown in Figure 11. A small (<<1%) amount of Fe has been added to the Mn-doped target. Fe preferentially substitutes for Ti and Fe concentrations of ~5% dramatically reduce the dielectric loss but at the same time, eliminate the dielectric tuning. Over the frequency range (1-20 GHz) and modest bias field examined (0 - 67 kV/cm), the deposited film exhibits ~ 8% tuning, however, the loss tangent is significantly reduced in comparison to the previous film. Dielectric Q's from 100 to 200 are seen up to 20 GHz. These are the largest Q's observed to date in films that exhibit significant tuning.

CONCLUSION

High quality, single phase, (100) oriented $Ba_{0.5}Sr_{0.5}TiO_3$ films were grown by PLD. Dielectric tuning and loss were measured from 1 - 20 GHz at room temperature and at 1 MHz as a function of temperature. These measurements showed that the dielectric properties could be significantly improved by annealing under the appropriate conditions. Precautions were needed to avoid the volatilization of elements in the films when annealed at temperatures above 1000° C. Bomb annealed films at temperatures as high as 1250 °C show an improvement in dielectric behavior. CSOM images indicate electrical inhomogeneties in the deposited films. BST films grown on $SrTiO_3$ exhibit behavior which is closer to the bulk single crystals, showing higher dielectric constants, a more sharply peaked temperature dependence, and lower dielectric losses, however, the temperature dependence of the phase transition is still sufficiently broad that ferroelectric switching is observed in nominally paraelectric (x=0.5) films. The most likely sources of the broadened transition temperature are nonuniform stress and compositional fluctuations across the sample. The film chemical stoichiometry was also shown to have a profound effect on dielectric properties. The addition of Mn (1-2 atomic %) has a dramatic effect on the dielectric loss. For modest bias fields (67 kV/cm) a ferroelectric thin film with 30% tuning and a dielectric Q of 100 ($\tan\delta$ - 1 x 10^{-2}) at room temperature (1 - 10 GHz) and 8% tuning with Q between 100 and 200 has been obtained. The data show that ferroelectric thin films can be used to make tunable microwave devices that have superior performance characteristics to devices fabricated from semiconducting materials at frequencies above 1 GHz.

ACKNOWLEDGMENTS

This work was supported by the Office of Naval Research and SPAWAR.

REFERENCES

1. V. K. Vardan, D. K. Ghodgaonkar, V. V. Vardan, J. F. Kelly, and P. Glikerdas, Microwave Journal **January,** 116-127 (1992).
2. J. S. Horwitz, D. B. Chrisey, J. M. Pond, R. C. Y. Auyeung, C. M. Cotell, K. S. Grabowski, P. C. Dorsey, and M. S. Kluskens, Integrated Ferroelectrics **8,** 53 (1996).
3. D. B. Chrisey and G. K. Hubler, *Pulsed Laser Deposition* (Wiley Interscience, New York, 1994).
4. K. Bethe and F. Welz, Mat. Res. Bull. **6,** 209-218 (1971).
5. K. R. Carrroll, J. M. Pone, D. B. Chrisey, J. S. Horwitz, and R. E. Leuchtner, Appl. Phys. Lett. **62,** 1854 (1993).
6. L. A. Knauss, J. M. Pond, J. S. Horwitz, D. B. Chrisey, C. H. Mueller, and R. E. Treece, Appl. Phys. Lett. **69,** 25 (1996).
7. A. C. Carter, J. S. Horwitz, D. B. Chrisey, J. M. Pond, S. W. Kirchoefer, and W. Chang, Integrated Ferroelectrics **17,** 273-285 (1997).
8. C. Hubert, J. Levy, A. C. Carter, W. Chang, S. W. Kirchoefer, J. S. Horwitz, and C. D.B., Applied Physics Letters **71,** 3353-3355 (1997).
9. S. B. Henner, F. A. Selmi, V. V. Varadan, and V. K. VArdan, Materials Letters **15,** 317-324 (1993).
10. N. H. Chan, R. K. Sharma, and D. M. Smyth, J. Electrochem. **128,** 1762 (1981).
11. D. R. Uhlmann, G. Teowee, and J. M. Boulton, J. Non-Crystalline Solids **131,** 1194 (1991).
12. R. Wasser, in *Ferroelecric Ceramics*, edited by N. Setter and E. L. Colla (Birkhause, Basel, 1993), p. 273.
13. W. A. Feil and B. W. Wessels, J. Appl. Phys. **74,** 3972 (1993).
14. H. P. R. Frederikse, W. R. Thurber, and W. R. Hosler, Phys. Rev. **134,** A442 (1964).

15. W. S. Baer, Phys. Rev. **144,** A734 (1964).
16. C. Lee, Y. Yahai, and J. L. Brebner, Phys. Rev. **B3,** 2525 (1971).
17. D. Wagner, D. Bäuerle, F. Schwab, M. Wöhlecke, B. Dorner, and H. Kraxenberger, Ferroelectrics **26** (1980).
18. S. B. Desu, Phys. Stat. Sol (a) **141,** 119 (1994).
19. C. Frenzel and H. Hegenbarth, Phys. Stat. Sol. (a) **23,** 517 (1974).
20. I. V. Barskii, O. G. Vendik, A. D. Smirnov, and G. S. Khizha, Sov. Phys. Tech. Phys. **34,** 1065 (1990).
21. D. R. Uhlmann, G. Teowee, and J. M. Boulton, J. Non. Crystalline Solids **131,** 1194 (1991).
22. S. S. Gevorgian, E. F. Carlsson, S. Rudner, U. Helmersson, E. L. L. Kollberg, a. E. Wikborg, and O. G. Vendik, .
23. T. S. Benedict and J. L. Durand, Phys. Rev. **109** (1958).
24. S. B. Herner, F. A. Selmi, V. V. Vardan, and V. K. Vardan, Materials Letters **15,** 317 (1993).
25. I. Burn, J. Mater. Sci. **14** (1979).